JOURNAL OF CATALYSIS 92, 79–97 (1985)

Infrared Study of ZnO Surface Properties: CO Adsorption and CO/D_2 Interaction at 77 K

GIOVANNA GHIOTTI, FLORA BOCCUZZI, AND ROBERTO SCALA

Istituto di Chimica Fisica, Università di Torino, Corso Massimo D'Azeglio 48, 10125 Turin, Italy

Received October 7, 1983; revised July 10, 1984

Infrared transmission spectroscopy has been used to study CO adsorption at 77 K on clean and D_2-pretreated ZnO surfaces. Two physisorbed species are present: one is localized on the free surface hydroxyls and the other is a liquid-like physisorbed species. Three CO chemisorbed species are detected, characterized by different chemisorption energies, as shown from the three different ranges of CO coverage in which they arise and reach their saturation. The comparison between CO adsorption on clean and D_2-pretreated samples shows that (i) the least energetic CO chemisorption occurs on the sites involved in the irreversible D_2 chemisorption, and (ii) the other two CO species involve sites interacting with the reversible D_2 chemisorbed species. Models for the chemisorption sites are proposed: consideration of the sites present on the $(10\bar{1}0)$, $(11\bar{2}0)$ and $(10\bar{1}1)$ faces allows us to explain the experimental data and to indicate their possible relevance for the synthesis of methanol.

INTRODUCTION

A number of adsorption studies of pure CO on ZnO powders at room temperature (RT) have been reported (*1–4*). Reversible adsorption occurs on Zn cations giving rise to an ir band with wavenumber in the range 2183–2191 cm^{-1}. The heat of adsorption is 44 kJ/mol and there is no apparent activation barrier for adsorption. Only 10% of surface is involved in this RT adsorption (*5, 6*).

H_2/CO (or D_2/CO) coadsorption on ZnO at RT has also been investigated (*6–10*). One such study was performed in our laboratory (*6*) with the aim of obtaining a more detailed description of the active sites for hydrogen chemisorption.

At RT two main processes of H_2 (or D_2) chemisorption have been identified, namely a rapid and reversible reaction, and a slow and irreversible one. The two different hydrogen chemisorbed species so formed have been designated type I and type II, respectively.

Type I chemisorption has been shown to be dissociative, giving rise to Zn–H and O–H groups. Recently the observation of bands due to irreversibly adsorbed hydrogen, which are associated with bridged OH–O and ZnH–Zn, structures have also been described, and a dissociative chemisorption process has been proposed for type II (*11*). Type II chemisorption has also been described as a diffusion of the adsorbate into the bulk (*12*).

H_2–CO or (D_2–CO) interaction at RT showed that CO is adsorbed on the same centers as those on which type I hydrogen adsorbs, producing well defined mixed CO–hydrogen structures. The adsorbing sites of H_2(I) and CO are suggested to be formed by a triplet of exposed zinc ions and at least one reactive oxygen ion. The continuous shift of the ν(ZnH) and ν(OH) frequencies with H_2(I) and CO coverage showed that these ion centers are not isolated, but are mutually interacting and grouped together forming a bidimensional array (*6*).

The reconstructed $(000\bar{1})$ and (0001) faces are shown to possess regular arrays of similar ion clusters (*6, 13*). Another suggestion (*14*) is that sites responsible for H_2(I) and CO coadsorption involve zinc ions carrying two unshared coordinative vacancies.

The ν(ZnH–Zn) and ν(OH–O) frequen-

0021-9517/85 $3.00

cies of type II hydrogen are completely unaffected by the presence of H_2(I) or CO (*6, 11*). This seems to imply that sites for type I and type II chemisorption are completely independent and that Zn ions involved in type II chemisorption no longer have coordinative vacancies to interact with CO at RT.

The aim of the present work is a more detailed characterization of the ZnO surface. The study of CO adsorption at low temperature (below room temperature) has been shown to be particularly useful for exhaustive characterization of an adsorbent (*13, 15–18*). In fact only a minor fraction of the surface is usually involved in room temperature adsorption, whereas the features of the whole surface can be revealed by weak interactions which take place at lower temperatures. The CO spectrum is then very sensitive to the nature of the sites, also in the case of very weak interactions.

Recent UPS studies of CO adsorbed at 77 K on ZnO single crystals showed that all the low index faces are able to adsorb this molecule with coverages very near to unity; the initial heat of adsorption (50 kJ/mol) decreases approximately linearly with coverage to about 20 kJ/mol at $\theta \simeq 1$ (*19, 20*). Ir and TPD studies of CO and H_2/CO adsorption at 100 K on ZnO powders (*13*) showed that a repulsive interaction exists between reversibly adsorbed CO molecules, while an attractive interaction exists between type I adsorbed H_2 and reversibly adsorbed CO.

Low temperature measurements have allowed us to study separately the interaction between CO and ZnO on which only D_2(I) or D_2(II) is preadsorbed. Data obtained in the two different experiments, compared with those of pure CO adsorption, have given us new interesting information about the nature of the sites responsible for the two types of adsorption and about the mechanism of activation of H_2 and CO as intermediates for reactions such H_2–D_2 exchange and CH_3OH synthesis.

EXPERIMENTAL

Two samples of ZnO were used in this study, the same as those employed previously (*6, 21, 22*): one was prepared by decomposing $ZnCO_3$ in a controlled atmosphere (BET surface area: 21 m^2/g) and the other was Kadox-25 zinc oxide (New Jersey Zinc Co.) prepared by combustion of zinc metal (BET surface area: 10 m^2/g).

Scanning electron micrographs have shown that the powders obtained by $ZnCO_3$ decomposition are formed of approximately monodisperse hexagonal prisms elongated along the *c* axis, while Kadox-25 is formed by larger and differently dispersed particles, of less defined shape (see Fig. 1).

The ZnO powder was compressed to obtain pellets of 2.5 cm diameter and of weight ranging from 0.2 to 0.4 g. The pellet was mounted in a suitable ir cell which allowed both heating and cooling (down to 77 K) in situ under vacuum (1×10^{-6} Torr, 1 Torr = 133.3 N m^{-2}) or under a controlled atmosphere. During ir measurements at low temperature some heating occurs at the center of the pellet, estimated approximately as 5–6 K.

Before each adsorption study the samples were cleaned by alternately outgassing in vacuo (1 h) and heating under 20 Torr of O_2 (10 min) three times at 673 K. After the last treatment, the samples were cooled to room temperature and evacuated down to 1×10^{-6} Torr. By this process the surface carbonate and water were mostly removed without loss of area or activity and a "quasistoichiometric" ZnO was obtained. The lowering of temperature to 77 K induces a decrease in the transparency of ZnO (*22*). For this reason all the results reported concern D_2 adsorption or CO–D_2 coadsorption, because both the Zn–D(I) and ZnO–D(I) stretching modes lie in regions of higher transparency than the corresponding Zn–H(I) and ZnO–H(I) stretching modes. Moreover, the ZnO–H(I) mode should superimpose on residual hydroxyl

bands of the zinc oxide, whereas this does not happen for ZnO–D(I). Measurements have been run as follows. After thermal treatments and oxygen evacuation at room temperature, the spectrum of the sample in 0.5 Torr of helium was recorded at 77 K. When it was necessary to preadsorb D_2 at higher temperatures, after recording the background at 77 K the sample was brought to the desired temperature and cooled back to 77 K.

All spectra were recorded with a Perkin-Elmer 580B spectrophotometer, the resolutions in the different regions examined being, respectively, 7.5 cm^{-1} in the 4000–3100 cm^{-1} range; 5 cm^{-1} in the 2700–2500 cm^{-1} range; 3.5 cm^{-1} in the 2200–2000 cm^{-1} range; and 2.5 cm^{-1} in the 1200–600 cm^{-1} range.

Scanning electron micrographs were made with a Coates and Welter scanning microscope.

RESULTS

CO Adsorption at 77 K

Typical spectra of adsorbed CO at 77 K on a ZnO sample obtained by $ZnCO_3$ decomposition are illustrated in Figs. 2 and 3. For CO equilibrium pressures lower than 1 Torr spectra were run on desorption, it being easier to reach the desired coverage by evacuation rather than by dosing in small CO quantities. Spectral modifications due to CO adsorption occur in the OH stretching region (3800–3000 cm^{-1}, Fig. 2a), in the OH bending and surface mode region (1000–600 cm^{-1}, Fig. 2b), and in the C≡O stretching region (2100–2250 cm^{-1}, Fig. 3a). Bold solid curves refer to the 77 K spectrum of the sample alone. Dashed curves are the spectrum run at 77 K when the sample is in contact with 5 Torr of CO.

In the OH stretching region the more prominent bands at 3670, 3625, and 3445 cm^{-1}, already assigned to surface free hydroxyls (*23, 24*), are destroyed and three new bands, broader and more intense, appear at 3630, 3580, and 3420 cm^{-1}.

In the lowest frequency region the transparency drastically increases between 750 and 600 cm^{-1} as a consequence of the disappearance of a band at about 720 cm^{-1} and of the erosion of the longitudinal optical absorption edge where ν(Zn–O) surface modes are present (*21*); simultaneously a new broad band appears at 800 cm^{-1}. In the CO stretching region two very intense and complex absorptions are visible. The first one, with a maximum at 2145 cm^{-1}, is definitely double; it shows in fact a shoulder at about 2136 cm^{-1}. The second one is a triplet of sharp bands, the most intense at 2169 cm^{-1}, the intermediate at 2178 cm^{-1}, and the third, visible only as a shoulder, at about 2187 cm^{-1}.

At equilibrium pressures higher than 5 Torr no change occurs in the hydroxyl and surface mode regions, while modifications are still visible in the CO stretching region, where only the component at 2136 cm^{-1} increases, but high increments in pressure (40, 100, 200 Torr) are necessary to obtain appreciable changes in its intensity. The difference in optical density (OD) between the two spectra at CO equilibrium pressures of 200 and 5 Torr (each with the gaseous phase spectrum subtracted) is reported in Fig. 3b. Only one band at 2136 cm^{-1} increases, with a half width of about 14 cm^{-1}.

The dot-dashed curve in Fig. 3a refers to 1 min evacuation (equilibrium pressure 1×10^{-2} Torr). The triplet at higher frequency is practically unchanged; the doublet at lower frequency drastically decreases, and a very sharp band at 2148 cm^{-1} remains with only a small shoulder; in the other two regions (Figs. 2a and b) this curve has not been reported so as not to overcrowd the figure. In the hydroxyl stretching region only the band at 3445 cm^{-1} is completely restored, the other stretching modes remaining still partially perturbed.

In the bending and surface mode region the band at 800 cm^{-1} partially decreases and that at 720 cm^{-1} partially increases, while the range 600–700 cm^{-1} remains com-

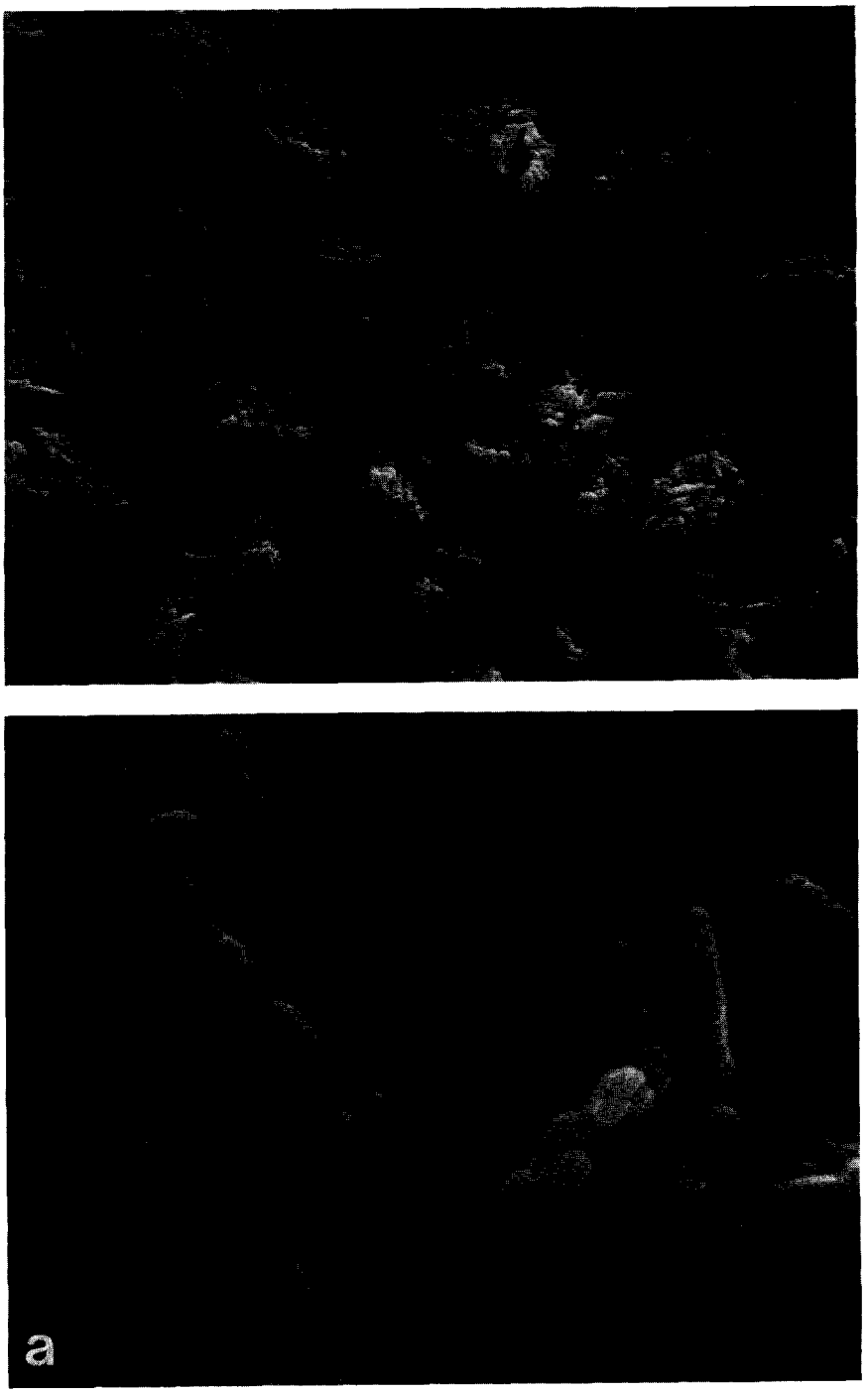

FIG. 1. Scanning electron micrographs of (a) ZnO ex carbonate,

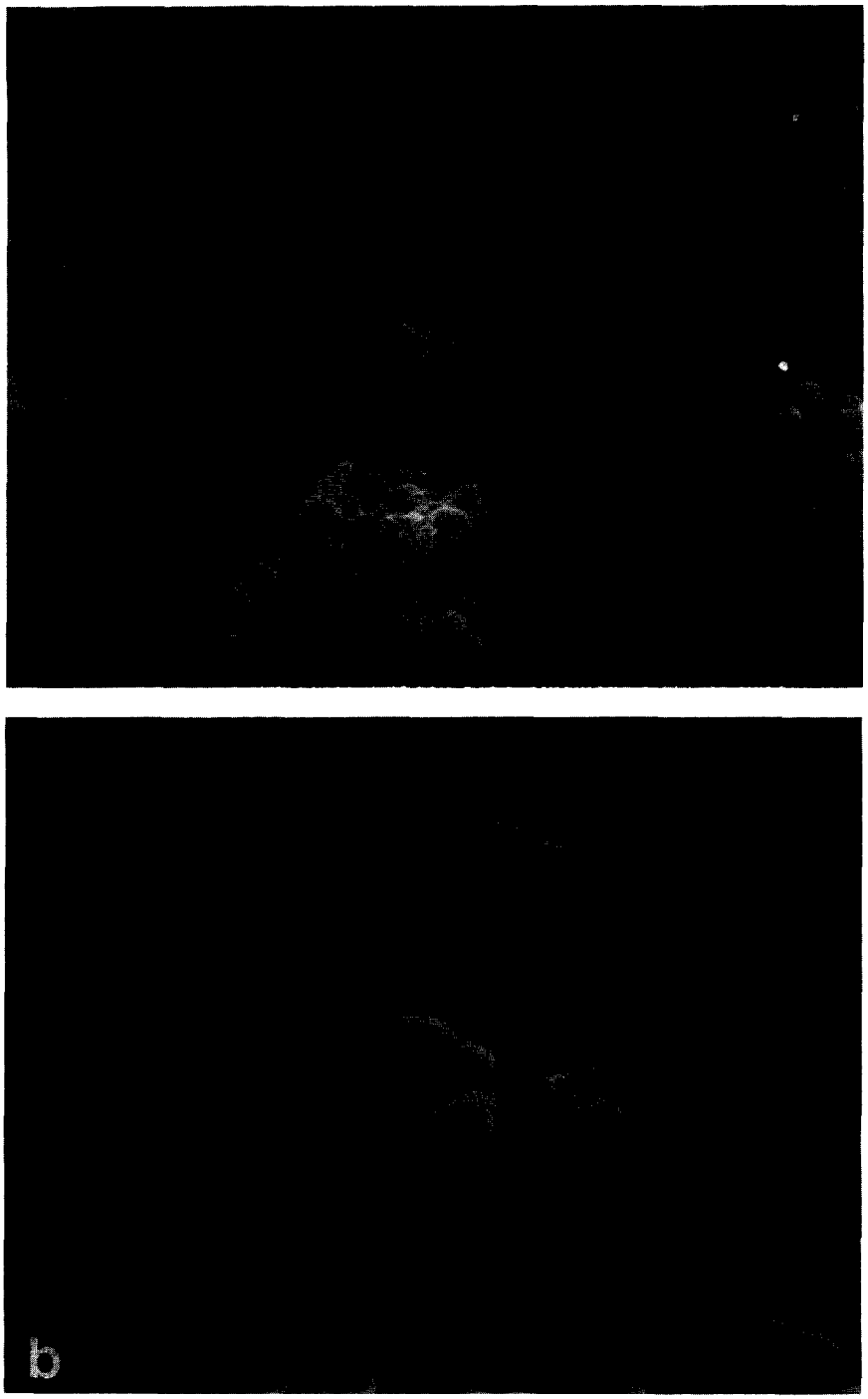

(b) Kadox-25. 20 kV. Top figures, ×15,000; bottom figures, ×50,000.

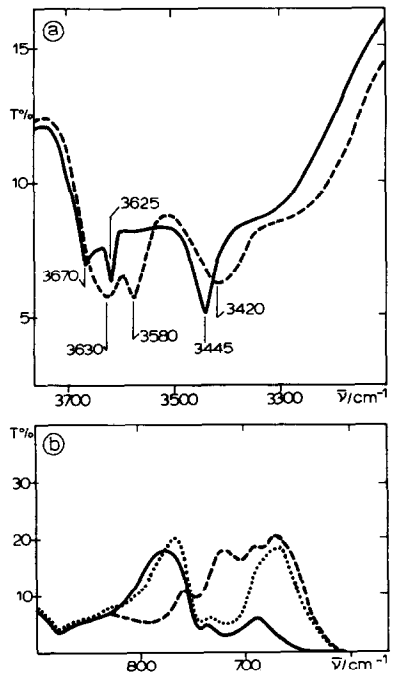

FIG. 2. CO interaction with ZnO (ex carbonate) at 77 K: (a) ν(OH) region; (b) δ(OH) and ν(ZnO) surface mode regions. Solid curves, background at 77 K; broken curves, 5 Torr of CO; dotted curve, after 2 min of evacuation.

pletely perturbed. Dotted lines refer to a 2 min evacuation: the band at 2148 cm^{-1} in Fig. 3 is practically destroyed, but no other variation is visible in the CO stretching region. In the OH stretching region (Fig. 2a) the spectrum is coincident with that of the clean surface (bold solid curve).

In the low frequency region (Fig. 2b) the 800 cm^{-1} band has disappeared and the 720 cm^{-1} band is completely restored. On the contrary the surface modes of the solid remain completely perturbed.

The other curves in Fig. 3a refer to different increasing times of evacuation. The first band of the triplet undergoing an intensity decrease is the 2169 cm^{-1} one, this intensity decrease being associated with an appreciable increase in frequency. The bands at 2178 and 2187 cm^{-1} are unaffected up to 6 min outgassing. For outgassing times higher than 6 min also the 2178 cm^{-1} band starts to decrease, shifting gradually toward higher frequencies. The shoulder at 2187 cm^{-1} is still visible and does not seem to decrease until 30 min outgassing. For outgassing times higher than 30 min only one band is present; its half-width is 12 cm^{-1} and its intensity decreases slowly with increasing evacuation times, regularly shifting from 2187 cm^{-1} toward higher frequency. After 90 min evacuation a very small band is still visible at 2193 cm^{-1}. For 6 min and higher evacuation times, variations are finally visible also in the range of the surface modes of ZnO (600–700 cm^{-1}), where the spectrum gradually regains the original absorbance. After 60 min outgassing the spectrum is practically coincident

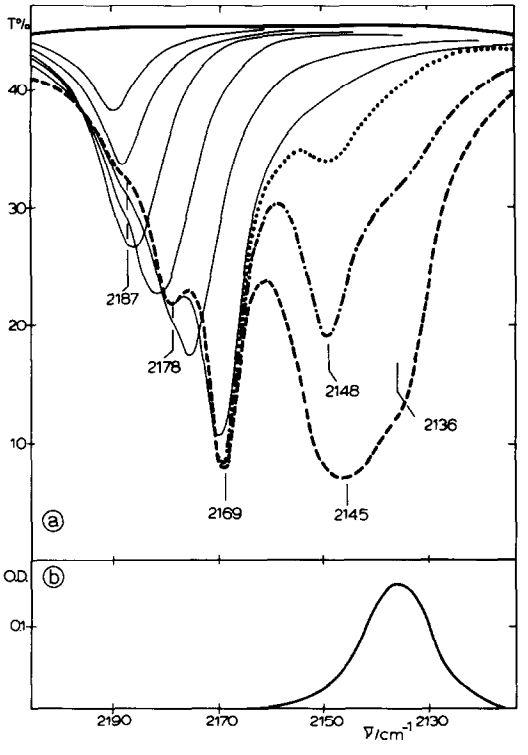

FIG. 3. CO interaction with ZnO (ex carbonate) at 77 K. ν(CO) region: (a) (transmission vs wavenumber) bold solid curve, background at 77 K; dashed curve, 5 Torr of CO; dot-dashed curve, after 1 min of evacuation; dotted curve, after 2 min of evacuation; thin solid curves, different increasing times of evacuation (4, 6, 15, 30, 60, and 90 min). (b) (optical density vs wavenumber) the difference between the two spectra at CO equilibrium pressure of 200 and 5 Torr.

with that of the clean sample (bold solid curve—Fig. 2b).

Results qualitatively similar to those just described are obtained when CO is adsorbed at 77 K on ZnO Kadox-25 samples. However, there is consistently a difference in the intensities of the triplet band (2169, 2178, 2187 cm^{-1}) for the two kinds of oxide, as illustrated in Fig. 4a. In this figure the spectra of CO adsorbed at a coverage corresponding to 2 min evacuation are reported for the two different oxides (OD vs cm^{-1}), these spectra being normalized to the surface unity area. If we make a comparison between any sample of ZnO obtained from carbonate and any one of Kadox-25, the difference in the two spectra is constantly in the direction noted in Fig. 4a:

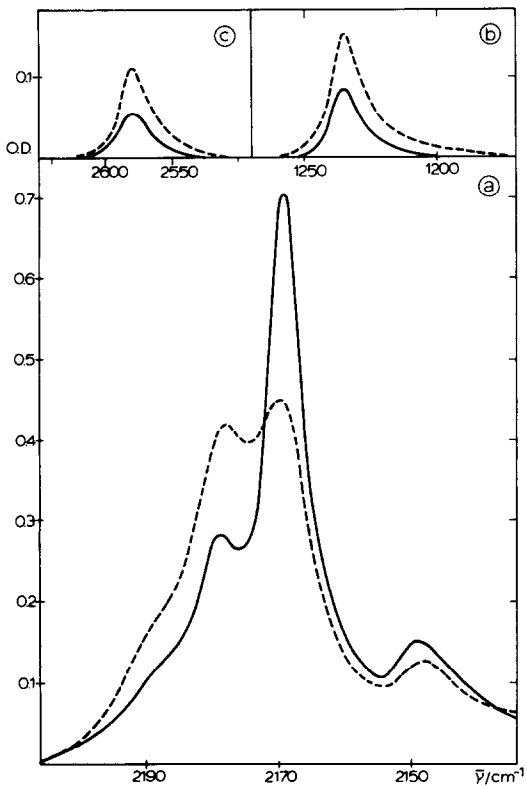

FIG. 4. Comparison between adsorption properties of ZnO ex carbonate (solid curves) and Kadox-25 (dashed curves). (a) CO interaction at 77 K (after 2 min of evacuation), ν(CO) region; (b) D_2 interaction at 195 K, ν(ZnD) region; (c) D_2 interaction at 195 K, ν(OD) region.

the ZnO Kadox-25 shows the pair of bands at 2178 and 2187 cm^{-1} to be more intense, and the band at 2169 cm^{-1} less intense than those of ZnO ex carbonate.

The interaction of CO at room temperature with the two types of ZnO produces only one band, highly pressure dependent, and whose position shows a red shift at increasing coverage. At an equilibrium pressure of 300 Torr, the band is at 2187 cm^{-1}, with a half width of 20 cm^{-1}. At this pressure the integrated optical density of this band is approximately the same as that of the band of CO adsorbed at 77 K with a coverage corresponding to 60 min of evacuation. This latter has a frequency and a half width of 2191 and 12 cm^{-1}, respectively.

We assume these results to be an indication of similar coverages at different temperatures. In that case, we can say that, at corresponding coverages, CO adsorbed at 77 K shows bands at higher frequency (5–6 cm^{-1}), and with a half width narrower than that of CO adsorbed at room temperature.

D_2 Adsorption

At room temperature (RT) type I adsorption is reversible and equilibrium data are obtainable; the saturation corresponds to an equilibrium pressure of about 100 Torr.

On the other hand type II adsorption at RT was found to be irreversible, so it must be the only species present on the surface, if after saturation in D_2 for 24 hr the ZnO is evacuated at RT for few minutes (*25*).

At low temperature, e.g., below 233 K, type I adsorption is irreversible and the amount of adsorption is kinetically controlled (*26*). At 77 K the D_2(I) coverage reaches only about 50% of the RT value within 15 min after the sample is exposed to 100 Torr of deuterium, but at 195 K the D_2(I) formation is still quite rapid and reaches saturation in a few minutes at the same pressure. The adsorbed quantity remains unaltered also after prolonged outgassing (*27*).

The solid line (OD vs cm^{-1}) in Figs. 4b, c refers to this last situation: the intensity and

the frequency of Zn–D stretching (1230 cm^{-1}) and O–D stretching (2585 cm^{-1}) are characteristic of saturated D_2(I) on any sample of ZnO Kadox-25, normalized to unit area. The same results are obtained on a sample of ZnO from $ZnCO_3$ (dashed line), but at corresponding surface area this type of sample constantly shows a minor activity toward D_2(I) chemisorption.

When D_2 adsorption was performed at 195 K or at lower temperature we never observed the formation of the bands characteristic of the D_2(II) species (*11*); this is proof that no ir detectable quantity of this species is formed, in agreement with volumetric adsorption measurements of Naito *et al.* (*26*).

Interaction $CO/D_{2\ ads.}$ at 77 K

As a consequence of the results illustrated in the preceding section it is possible to obtain ZnO surfaces with only one type of D_2 (or H_2) chemisorbed. We therefore studied separately the two different interactions, CO/D_2(I) and CO/D_2(II), respectively, at 77 K. In the first case the samples were contacted with D_2 (100 Torr, 10 min) at 195 K, then outgassed for few minutes and frozen at 77 K. In the second case the samples were contacted with D_2 (100 Torr, 24 hr) at RT, then evacuated for few min and frozen at 77 K. On the samples treated in the two different ways, CO was adsorbed at different coverages. As before, CO equilibrium pressures lower than 1 Torr were reached by desorption.

In Fig. 5a a comparison between the spectra of CO adsorbed on a clean surface (solid curve) and on a surface with D_2(I) preadsorbed (dashed curve) is illustrated for the CO stretching region. The sample is ZnO Kadox-25, the CO equilibrium pressure is 5 Torr. As far as the triplet at higher frequency is concerned, the peak at 2169 cm^{-1} is unchanged in frequency and intensity, while the two components at 2178 and 2187 cm^{-1} are replaced by two others, higher in intensity and frequency (2180 and 2190 cm^{-1}). The doublet at lower frequency

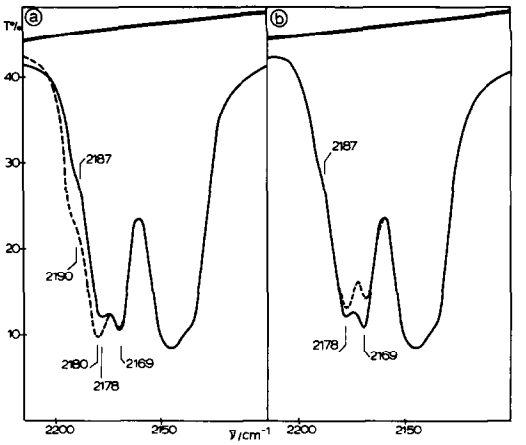

FIG. 5. Comparison between CO interaction at 77 K (5 Torr) with clean ZnO (Kadox-25) and with ZnO (Kadox-25) with preadsorbed D_2: ν(CO) region. (a) CO/D_2(I) interaction; (b) CO/D_2(II) interaction. Bold solid curves, background at 77 K; thin solid curves, CO interaction on clean surface; dashed curves, CO interaction after D_2 adsorption.

(2148, 2136 cm^{-1}) remains unperturbed. Figure 5b shows the behavior of the CO bands in the case of the preadsorbed D_2(II). The 2169 cm^{-1} peak shows a notable intensity decrease but its frequency remains unchanged. No variation in intensity and frequency is shown by any of the other components.

In Figs. 6, 7, and 8 the change of the spectrum with CO coverage is illustrated for the case of CO/D_2(I) interaction.

Sections (a) refer to the CO stretching region, sections (b) and (c) to ν(Zn–D) and ν(O–D) regions, respectively. The changes of the spectrum in the 4000–3200 and 1000–600 cm^{-1} regions are not reported, as they are the same as observed in the CO/clean surface interaction.

Bold solid curves in Fig. 6 refer to the spectrum of the sample with only preadsorbed D_2(I). Bold dashed curves refer to the spectrum run when the sample is in contact with 5 Torr of CO. The CO stretching region of this spectrum was previously described (Fig. 5a). At this coverage the CO adsorption broadens and shifts the ν(Zn–D) band to lower frequency, from 1232 to 1187 cm^{-1} ($\Delta\bar{\nu} = -45\ cm^{-1}$), but leaves its inte-

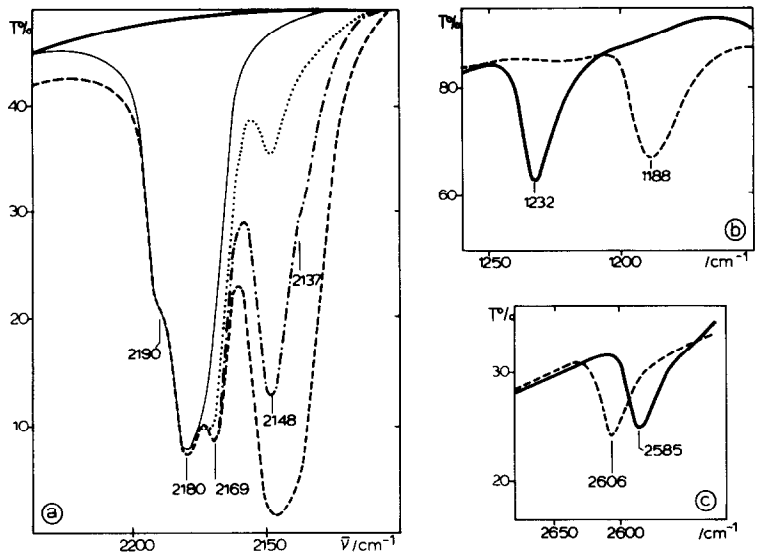

FIG. 6. CO interaction at 77 K on ZnO (Kadox-25) with preadsorbed D_2(I): (a) ν(CO) region; (b) ν(ZnD) region; (c) ν(OD) region. Bold solid curves, ZnO with preadsorbed D_2(I); dashed curves, 5 Torr of CO; dot-dashed curve, 1 min of evacuation; dotted curve, 3 min of evacuation; Thin solid curve, 7 min of evacuation.

grated intensity practically unperturbed. The effect on the ν(O–D) is a notable shift toward higher frequency, from 2856 to 2606 cm^{-1} ($\Delta\bar{\nu}$ = +50 cm^{-1}), leaving the intensity unchanged. The other curves in Figs. 6, 7, and 8 refer to increasing evacuation times.

As for the CO stretching region we observe that the two components at 2180 and 2190 cm^{-1} show the same behavior as the 2178 and 2187 cm^{-1} components (present on the clean surface). In fact they remain unchanged in intensity and frequency in the first desorption range (5 Torr—7 min of

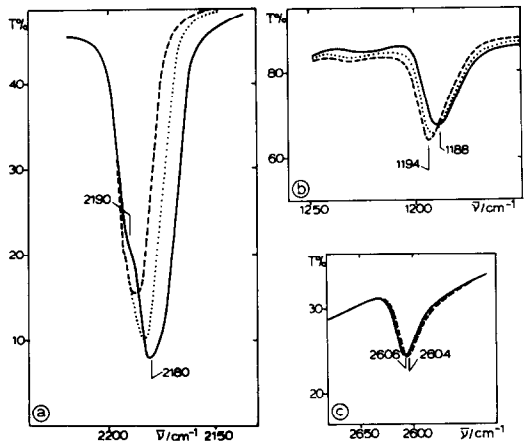

FIG. 7. CO interaction at 77 K on ZnO (Kadox-25) with preadsorbed D_2(I): (a) ν(CO) region, (b) ν(ZnD) region; (c) ν(OD) region. Thin solid curves, 7 min of evacuation (the same as in Fig. 6); dotted curves, 13 min of evacuation; dashed curves, 15 min of evacuation.

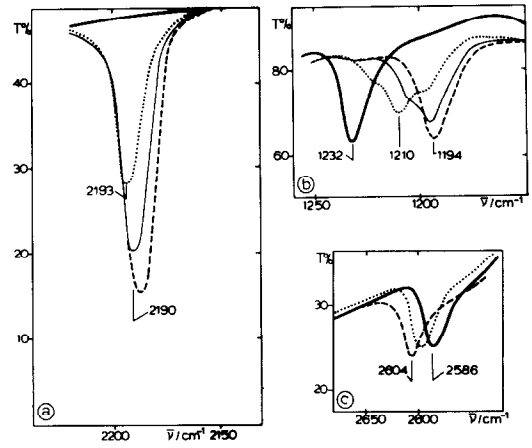

FIG. 8. CO interaction at 77 K on ZnO (Kadox-25) with preadsorbed D_2(I): (a) ν(CO) region; (b) ν(ZnD) region; (c) ν(OD) region. Dashed curves, 15 min of evacuation (the same as in Fig. 7); thin solid curves, 35 min of evacuation; bold solid curves, ZnO with only preadsorbed D_2(I) (the same as in Fig. 6).

evacuation); the 2180 cm^{-1} component decreases in intensity and shows a blue-shift in the second desorption range (7–30 min of evacuation), while the 2190 cm^{-1} one shows this behavior for desorption times greater than 30 min.

As regards the other two spectral regions, we observe that in the first desorption range, corresponding to the disappearance of the 2136, 2148, and 2169 cm^{-1} bands, the ν(O–D) and ν(Zn–D) bands are unperturbed. In the second desorption range, corresponding to the 2180 cm^{-1} disappearance, small blue-shifts of the ν(Zn–D) from 1188 to 1194 cm^{-1} are observed together with a weak sharpening, while only a very small (2 cm^{-1}) red shift of the ν(O–D) band is observed. In the third desorption range, corresponding to the disappearance of the 2190 cm^{-1} component, the ν(Zn–D) at 1194 cm^{-1} decreases with a continuous blue-shift. At the same time a band at higher frequency (~1210 cm^{-1}) appears and reaches its maximum after about 60 min evacuation. It then decreases while a third band at higher frequency appears. The frequency and intensity of this band continuously increase with decrease of the CO coverage, moving toward those of the ν(Zn–H) band before the CO contact (1232 cm^{-1}). Meanwhile the ν(O–D) band shows a continuous red frequency shift towards the original frequency at 2586 cm^{-1}. This behavior is inverse to that occurring when at RT CO is allowed to bleed in on a hydrogen-saturated sample (i.e., in equilibrium with 100 Torr of D_2) to give gaseous mixtures (*6*).

In the case of the CO/D_2(II) interaction, the change of the spectrum with decreasing CO coverage is the same as is observed for CO adsorbed on a clean surface (figure not reported).

Interaction D_2/CO_{ads} at 77 K

The interaction was studied for all CO coverages reported in Fig. 3a.

The experiment was performed as follows: the sample with a given coverage was contacted with 100 Torr of D_2 at 77 K for 15 min and then briefly evacuated. No type I chemisorption was observed until coverages lower than that corresponding to 6 min evacuation were reached. For coverages corresponding to evacuation times higher than 6 min and lower or equal to 30 min we observed a blue shift of the two bands still present in the CO stretching region and the appearance of the ν(Zn–D) mode at 1187–1194 cm^{-1} and the ν(O–D) mode at 2606–2604 cm^{-1}, in their lower and higher position respectively. The two bands reached their maximum intensity for the coverage corresponding to about 30 min evacuation. For CO coverages corresponding to evacuation times higher than 30 min, the contact with D_2 still produced a blue shift of the single CO stretching band now present, while in the ν(Zn–D) region a doublet or a triplet of bands appeared and the ν(O–D) mode was at lower frequency.

DISCUSSION

Physisorbed CO

Among the five components present in the CO stretching region the assignment of the two bands at 2136 and 2148 cm^{-1} is the most simple: the lability immediately suggests they correspond to physisorbed species. The first one has a position characteristic of a condensed CO phase, and its presence does not perturb any other spectral region, showing that it is due to a nonspecific liquid-like physisorption. The second band has a frequency higher than that of the gaseous phase and perturbs the free hydroxyls of the surface. It causes a shift to lower frequency and an enhancement of the OH stretching modes (from 3670, 3625, 3445 cm^{-1} to 3630, 3580, 3420 cm^{-1}, respectively) together with a shift to higher frequency of the bending modes (from about 720 to 800 cm^{-1}), as expected when hydrogen bonds are formed. This physisorbed species is therefore localized on free hydroxyls of the surface, as already observed in the case of silica (*15, 16*).

Chemisorbed CO

The assignment of the other three components is not immediate. In the first instance they can be assigned to three different CO chemisorbed species: CO(1), CO(2), and CO(3), corresponding respectively to the 2169, 2178, and 2187 cm^{-1} bands, involving different interaction energies, as shown from the three different ranges of coverage in which the three components appear and reach their maximum intensity. The chemisorbed species corresponding to the component at higher frequency is the only one to involve a chemisorption energy higher than thermal energy at room temperature (RT). In fact only one band is visible for CO adsorption at RT; its intensity markedly depends on the equilibrium pressure and its position continuously shifts to higher frequency as coverage decreases. This band shows a half-width larger than the corresponding one at low temperature, and is shifted to lower frequency, according to what happens to the stretching modes of other carbonyl surface species (*17*).

D_2 and CO Coadsorption

We can confirm these assignments and give a more detailed description about the sites involved in the chemisorption from the study of CO interaction with preadsorbed D_2. Both D_2(I) and D_2(II) preadsorbed modify the spectrum of chemisorbed CO, but in different ways.

D_2(II) preadsorption decreases the 2169 cm^{-1} component, revealing competition of CO(1) and D_2(II) for the same sites. The other two components are not perturbed, so we can say that their sites are not sites for D_2(II) adsorption. D_2(I) preadsorption leaves the 2169 cm^{-1} component unperturbed but intensifies and slightly shifts the other two components to higher frequencies. It follows that the sites for the 2169 cm^{-1} species are not sites for D_2(I) adsorption. The other two species evidently interact with D_2(I) but it is not easy to understand immediately how. These interactions can be clarified by the study of CO desorption in the three spectral regions of Figs. 6, 7, and 8.

As noted in the Results section, the bands at 2180 and 2190 cm^{-1} show the same behaviour as the 2178 and the 2187 cm^{-1} bands. We therefore regard them as due respectively to the CO(2) and CO(3) chemisorbed species, perturbed by the D_2(I), the effect of the perturbation being practically the same for the two bands. On the other hand the same experiment suggests that while CO(3) chemisorbed species produce the greater perturbations on ν(Zn–D) and ν(O–D), the subsequent formation of chemisorbed CO(2) only slightly perturbs these modes. The great perturbations in the ν(Zn–D) and ν(O–D) region were previously assigned by some of us (*6*) as due to different adsorption steps occurring on Zn ion triplets. Thus it is clear that only the CO(3) chemisorbed species are responsible for these mixed complexes.

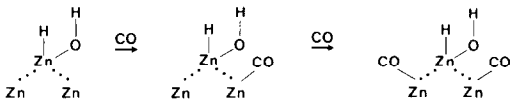

Moreover, from the experiments illustrated in the last paragraph of the Results section it is evident that D_2(I) cannot be formed when the coverage in CO(2) chemisorbed species is complete. Decreasing the CO(2) coverage brings about increasing D_2(I) adsorption, while the ν(Zn–D) and ν(O–D) frequencies for all CO(2) coverages remain those of the mixed complex richer in CO. The characteristic frequencies of the complexes poorer in CO appear only when the CO(3) coverage begins to decrease. This is a proof that when saturation in CO(3) species is verified, sites for D_2(I) adsorption are completely bare. On the other hand, although CO(2) is not responsible for the mixed complexes, it inhibits in some way the D_2(I) chemisorption.

Inductive Interactions

All bands of the adsorbed species on ZnO show frequency shifts at increasing coverages.

Coverage-induced frequency shifts in vibrational spectra of adsorbed molecules can be induced either by dynamic or by static interaction between molecules. Dynamic shifts are attributed to electrodynamic interactions between oscillating dipoles, and act only between isotopically similar adsorbates (e.g., CO–CO, ZnH–ZnH). Static shifts may be caused either by electrostatic or by chemical interaction, or both, and the magnitude of these interactions determines the adsorption energy change. Recently Griffin and Yates (*13*) have described a method of calculation of both dynamic and electrostatic shifts for the bands of the CO and H_2(I) chemisorbed species on ZnO. They computed the chemically induced shifts as the difference between the observed shifts and the predicted electrostatic and dynamic shifts (when present). They concluded by offering a qualitative explanation for the latter quantity, based on the inductive interactions between adsorbates.

Following Griffin and Yates, the dissociative H_2(I) adsorption is an electron-localizing process with regard to electron density initially present at a vacant site, and we are in agreement with this statement. As a consequence "H_2 adsorption will decrease the available electronic density at the neighboring sites (i.e., it will have a negative sigma-inductive effect)", providing a good explanation of the ν(Zn–H) and ν(Zn–OH) frequency shifts with H_2 coverage. In fact a negative sigma-inductive effect will slightly increase the positive charge on the neighboring zinc atoms and slightly decrease the negative charge on neighboring oxygen atoms. The Zn–H bond will become more covalent at increasing H_2 coverage with a higher stretching frequency; the O–H bond will be less covalent, and the frequency will shift toward lower values. This is well supported by the effect due to the introduction of different sigma-inductive groups on the ν(XH) of a series of hydrides and of a series of alcohols and acids (*28*), where it is evident that a sigma-inductive negative group decreases the hydroxyl stretching frequencies, while the hydride stretching frequencies increase.

Again following Griffin and Yates the inductive interaction provides an equally straightforward explanation of the frequency shifts for H_2–CO and CO–CO interactions. CO adsorption on ZnO is an electron-donating process occurring out of the weakly antibonding 5σ CO orbital. As a consequence it will increase the available negative charge at the neighboring sites (i.e., it will have a positive sigma-inductive effect). This provides a good interpretation of the red shifts of CO stretching modes at increasing CO coverages. In fact "a neighboring CO_{ads} molecule should inhibit the extent of 5σ electron donation by a reference CO_{ads} molecule." Since the 5σ orbital is weakly antibonding, decreased electron donation should weaken the C≡O bond, and thus decrease the CO stretching frequency. We agree with this interpretation; however, we have been able to resolve into three components the CO stretching band considered as unique by these authors.

If we consider the frequency shifts in ν(Zn–H) and ν(ZnO–H) due to adsorbed CO, we predict that the presence of an electron-donating adsorbed CO molecule at a neighboring site will decrease the positive charge on a Zn ion and increase the negative charge on an oxygen ion at the reference H(I) adsorption site, so the covalence of the Zn–H(I) bond will be lowered and that of the ZnO–H(I) bond will be raised according to the observed shift.

Finally we must consider the frequency shift of the CO stretching modes due to the σ inductive negative effect caused by preadsorbed H_2. As expected, the CO(2) and CO(3) stretching frequencies increase. No effect is observed on the CO(1) frequency.

Surface Sites on ZnO

The picture we can infer so far can be summarized as follows:

(i) There is some heterogeneity of surface sites on ZnO; there is evidence for four different Zinc ion families, which we will label as A, B(1), B(2), and C sites. A sites are responsible for CO(1) and D_2(II) adsorption. B(1) sites are responsible for D_2(I) adsorption. B(2) sites are responsible for CO(3) adsorption and are nearest neighbors to B(1) sites. C sites are responsible for CO(2) adsorption, their structure and orientation with regard to B(1) sites being such that a CO molecule preadsorbed on them inhibits the D_2(I) chemisorption.

(ii) The continuous shift of frequencies with coverage of the bands corresponding to all chemisorbed species shows that the different sites are not isolated, but lie on regular portions of surface. Moreover, while B(1), B(2), and C sites must be on the same regular portions of a face, A sites must lie on regular portions of a different face. More precisely, B(1) and B(2) sites must be on the same regular array, C on adjacent arrays.

(iii) All the three CO chemisorbed species are active in destroying the absorption due to the vibrational surface states of the solid (700–600 cm^{-1}). A more detailed examination of the different components of this absorption and of their dependence on the CO chemisorbed coverage would be useful in order to clarify the nature of the involved sites. We hope to continue work along this line.

The Models

No models have been proposed up to now for sites chemisorbing D_2(II), although models of the ZnO surface that provide Zn ion triplets for D_2(I) and the successive formation of mixed complexes with CO have been suggested. One of these (*6*), proposed by some of us, is a reconstructed (2 × 2) ZnO (000$\bar{1}$) surface in which one quarter of the O anions have been removed. Griffin and Yates (*13*) proposed a (2 × 2) reconstructed ZnO (0001) surface in which one quarter of the Zn cations have been removed. Lavalley *et al.* (*14*) proposed a new model on the basis of results obtained using CO_2 as a probe molecule, showing the presence of particular sites on ZnO which can be described as surface zinc ions with two vacancies, with a basic oxygen in an adjacent position. They proposed (*29*) the same model for the H_2/CO interaction. We think, however, that none of these models is sufficient to explain all the observed low temperature phenomena, in particular the presence of two distinct sites on the same face for CO adsorption, and the inhibition effect shown by CO(2) species toward D_2(I) chemisorption.

Before we propose a new surface model, it is useful to remember the differences always shown by the two ZnO samples examined (ZnO Kadox-25 and ZnO from decomposition of carbonate) illustrated in the Results section. On the basis of the analysis carried out up to now, we can say that for the same surface area the portions of regular surface carrying A sites, compared with those carrying all the others, must be greater in extent on the ZnO ex carbonate than on the Kadox-25. Starting from the reasonable hypothesis that CO at 77 K covers almost all the surface, the observed differences may be ascribed to some differences in the ratio between the more exposed faces on the two ZnO samples examined. In fact electron micrographs show that powder obtained by $ZnCO_3$ decomposition is formed of well-defined prismatic particles, whilst the powder of Kadox consists of less-defined, wider and shorter particles; thus we can infer that ZnO ex carbonate exposes a greater amount of prismatic faces. The less-defined shape of the Kadox particles may be interpreted as due to the exposure of faces of higher index obtained from a continuous succession of steps formed by polar and nonpolar low index faces (as happens on pyramidal faces).

We can therefore test the following

models for H_2 and CO chemisorption: (1) H_2(II) or D_2(II) and CO(1) species involve sites present on nonpolar prismatic faces like $(10\bar{1}0)$ and $(11\bar{2}0)$, as illustrated in Fig. 9. However, we think that the $(10\bar{1}0)$ face is the only one able to give the H_2 or D_2(II) chemisorbed species; the nature of the vibrational modes related to this species (*11*) indicates that it is formed of a bridged hydride and a bridged hydroxyl group. Only the $(10\bar{1}0)$ face can offer pairs of Zn ions and oxygen ions with uncoordinated vacancies oriented in a suitable direction. On the other hand, we think that the two surfaces are equally able to adsorb CO with very similar interaction energies, as demonstrated by Gay *et al.* (*19*). The presence, on the $(11\bar{2}0)$ face, of sites A only capable of chemisorbing CO but not of dissociating H_2 into H_2(II) species, may be the reason for the constant presence, on samples which preadsorbed H_2 at RT, of a considerable fraction of CO(1) adsorbed species, with a CO stretching frequency not perturbed by the H_2(II) coverage.

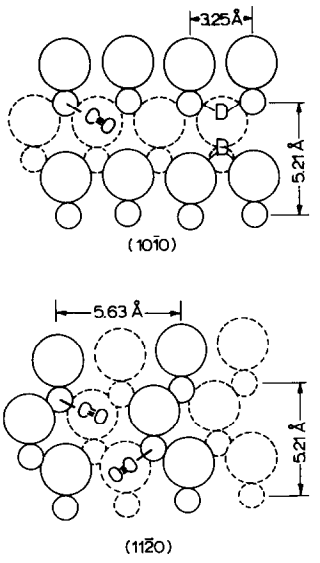

FIG. 9. Surface geometry of the $(10\bar{1}0)$ and $(11\bar{2}0)$ faces of ZnO and model for CO(1) and D_2(II) chemisorption. Large circles, oxide ions; small circles, zinc ions. Solid circles, surface layer; dashed circles, second layer.

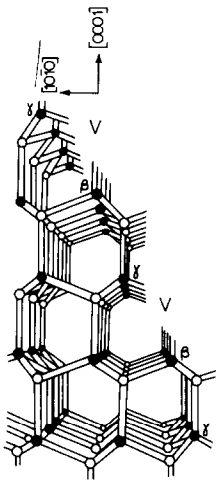

FIG. 10. Model of a stepped $(10\bar{1}1)$ face of ZnO. Solid circles, zinc ions; open circles, oxide ions.

(2) H_2 or D_2(I), CO(2), and CO(3) species involve sites present on pyramidal faces. One of these, the hexagonal $(10\bar{1}1)$ face, seems to be particularly suitable as our model. We notice that this is still a low index face, and thus has a higher probability to be exposed. On this plane two face-to-face rows of uncoordinated zinc ions are present, which we label as β and γ Zn ions, essentially different in the orientation of their dangling bonds with respect to the surface plane (*30*). This is evident in the perspective drawing of Fig. 10, where these dangling bonds are shown and where the letter V represents, for sake of clarity, the position of the row of missing anions. Moreover, each Zn-ion double row is separated from its neighbor by a row of uncoordinated oxygens bridged between a β and a γ Zn ion.

Another pyramidal face is the $(11\bar{2}1)$ face, on which two face-to-face rows, one of threefold and the other of twofold coordinated Zn ions, are present. Although we cannot exclude the presence of this face, it will certainly be less probable than the $(10\bar{1}1)$ face, simply because only zinc ions with one uncoordinative vacancy are present on this latter.

The CO(2) and CO(3) chemisorbed spe-

cies. We consider that when a CO molecule is put into contact with the clean $(10\bar{1}1)$ face, it will be attracted by the electrical field of the two face-to-face zinc ions, but at the moment of the bond formation the electronic properties and the geometry of the system is critical for the structure of the chemisorbed species. In fact the two Zn ions are separated by about 3.25 Å and no bridged species can be formed, as in fact the experiment shows. Thus the CO molecule, to minimize better the energy of the system, will adsorb to saturate only one sp^3 dangling bond of the two face-to-face Zn ions. As a consequence of the different orientation of the dangling bonds with respect to the surface plane, two different linear carbonyl species can be formed, one arising from a β type and the other from a γ type dangling bond saturation (see Scheme I).

To appreciate better the structure of the two possible chemisorbed species it is useful to keep in mind the average bond distances of some linear homogeneous carbonyl complexes, in particular those of Cu, which can be taken in this case as a suitable reference system and where the metal–carbon bond is ~1.8 Å long and carbon–oxygen distance is ~1.14 Å (*31*). Hence the Zn–C bond distance should certainly be no shorter than 1.8 Å, and probably a little longer, and it should be very near to the zinc–oxygen distance bond of zinc oxide itself, which is 1.91 Å. In the two species the carbon atom could be imagined to occupy a surface position very near to that of the missing surface oxygen, the V position of Scheme I. On the other hand, if the sigma bond is formed with the β zinc ion, the oxygen end of the bond (i.e., the positive end of the dipole) is localized on the plane formed by the C≡O bond itself and the dangling bond from a surface uncoordinated oxygen, in such a way as to allow attractive interaction. This attraction can be considered to be synergetic with the carbon–metal sigma bond formation and thus there is an increased stretching frequency with respect to the situation where the CO molecule is attracted only by a zinc ion.

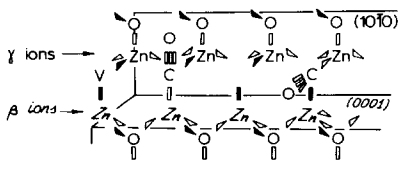

SCHEME I

If the second type of interaction (that with the γ zinc ion) is kept under consideration, the direction of the saturated Zn dangling bond is such that the C≡O bond protrudes out of the surface, while the oxygen bond is away from the two neighboring uncoordinated surface oxygens, on a plane different from those that contain oxygen dangling bonds, where the negative charge is mainly localized. The attractive interaction will be weaker.

We therefore believe that the most energetic CO(3) species, which has the highest ν(C≡O) frequency (2187 cm^{-1} at maximum coverage) is that adsorbed on β ions, which can be made coincident with the B(2) sites.

The adsorption of the first molecule will produce a sigma-inductive positive effect on the other surface Zn ions. This effect will be maximum on the two nearest neighbor β ions, which are separated only by an oxygen–zinc bond, but will be very weak on the face-to-face γ zinc ion from which it is separated by three oxygen-zinc bonds. The probability that two β neighbors adsorb CO is very poor. At a certain coverage the σ-inductive effect on the β ions still bare will be such that the adsorption on γ sites will be practically the same or more energetic, and so the CO(2) species will be formed ($\bar{\nu}$ = 2178 cm^{-1}, at maximum coverage) and γ ions can be identified with C sites.

For sake of clarity and simplicity we show in Scheme II an ideal ordinate situation where only one CO molecule is adsorbed per two Zn ions, with an alternative orientation, one of β and one of γ type.

The H_2(I) chemisorbed species. We also propose that β zinc ions are the positive

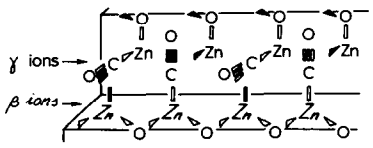

SCHEME II

partners of the sites for H_2(I) adsorption, while the upper oxygens are the negative partners of this dissociative adsorption, the mechanism of the reaction being illustrated in Scheme III. The hydrogen molecule, strongly polarized by the electric field of the two face-to-face zinc ions and oriented with its induced positive pole toward the upper oxygen anion, can dissociate, producing H_2(I) chemisorbed species. Owing to the sigma-negative inductive effect, this H_2 adsorption occurs only on one half of the zinc–oxygen couples. Thus we have identified the structure of the B(1) sites. Nevertheless, from this discussion it is evident that the zinc ions responsible for CO(3) and the hydridic part of the H_2(I) species are structurally the same, so that the distinction between B(1) and B(2) sites is not necessary to explain the experimental data. Hence from now on we will refer only to B sites.

The mutual position of Zn–H(I) and OH(I) partners is such that their recombination to give a hydrogen molecule (the desorption process) can easily take place during an elongation of the Zn–H bond in its stretching vibration and a contemporaneous decrease of the Zn–O–H angle during the OH bending vibration, as illustrated by the arrows in Scheme III. The model is consistent with the reversibility of the H_2(I) species at RT.

The interaction D_2/CO. The CO interaction with preadsorbed H_2(I) or D_2(I) will first saturate the B ion nearest neighbors and afterward the face-to-face C ions, as shown in Scheme IV. The latter are evidently still bare for CO adsorption. This is in agreement with the fact that the H_2 is strongly polarized by the zinc B ion to make a Zn–H(I) bond partially covalent, its length being very near to that of molecular zinc hydrides (1.62 Å), as supported by the high ν(Zn–H) frequency values, nearly coincident with that of the molecular zinc hydrides (1695 cm^{-1}) (*32*). Its formation leaves space enough for the CO molecule. Moreover, this model is compatible with the same effect produced by the presence of H_2(I) species on the frequencies of the CO(2) and CO(3) chemisorbed species. In fact at saturation of H_2(I) or D_2(I) a CO molecule adsorbed either as CO(3) species or as CO(2) species is coordinated to zinc ions directly bonded to the hydroxyl partner of the H_2(I), i.e., the part of this adsorbed species where is mainly localized the electronic charge extracted from the solid. Thus the two zinc ions become equally impoverished of electron density and as a consequence an equal enhancement of the sigma bond must be expected, that is an equal shift in the C≡O stretching frequencies of the two species (2178 → 2181 cm^{-1}, 2187 → 2190 cm^{-1}).

As far as the different effect of the two CO chemisorbed species on the ν(Zn–H) and ν(ZnO–H) is concerned, the model is well consistent with what happens.

Let us discuss first the effect of the CO(3) species, the more energetic one. From Scheme V it is clear that while it is possible

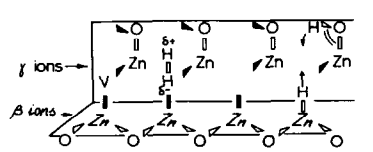

SCHEME III

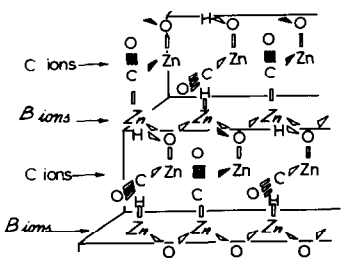

SCHEME IV

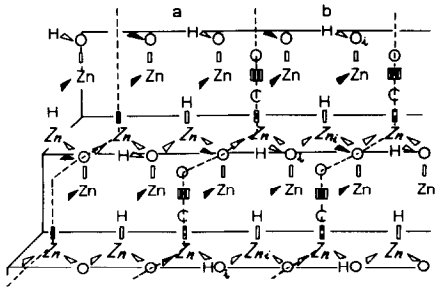

SCHEME V

to speak of two equivalent nearest neighbor CO(3) molecules for any Zn–H group kept as a reference, it is possible to speak of only one nearest neighbor CO(3) species for any Zn(O–H) species kept as a reference. In fact in this model the zinc ion triplets are the repetitive unit of a chain delineated in Scheme V by the dashed line. Passing from low to high CO(3) coverage, the entry of the second CO molecule into the triplet gives rise, as regards Zn–H, to a second CO(3) carbonyl equivalent to the first one. On the contrary, the entry of the second CO(3) molecule into the triplet is not equivalent to the first one as regards the OH partners. This second molecule will be the nearest neighbor of another hydroxyl, so, while discontinuous shifts are expected for the Zn–H species, only continuous shifts are expected for the OH species.

Let us now comment on the subsequent effect due to the CO(2) species. The small but visible effect on the ZnH species is probably caused by the electrostatic interaction due to the extreme proximity of the two species. As for the very small effect on the ν(O–H) frequency, it can be ascribed to the very weak sigma bond involved in this interaction.

Finally the model also accounts for the inhibition effect of the CO(2) preadsorbed species with respect H_2(I) adsorption. When the CO(2) coverage on a surface is complete, all the face-to-face Zn ions are screened by CO(2) or CO(3) species. There is not a positive electric field sufficiently intense to polarize the H_2 molecules. Only when some CO(2) species are desorbed giving rise to some face-to-face completely bare zinc pairs can the adsorption take place; only dicarbonyl mixed complexes can be formed until the CO(3) coverage is maximum. On the other hand, the presence of the CO(3) species at maximum coverage should leave completely unaltered the capacity of the surface for adsorbing H_2, or even should favor it, from an energetic point of view, owing to the opposite sigma-inductive effect that they exercise on the solid.

Reaction Mechanisms

Type I chemisorbed H_2 was demonstrated (*33*) to participate directly in catalytic reactions such as D_2–H_2 exchange and ethylene hydrogenation, and was proposed (*34*), very reasonably, to be one of the intermediates in the methanol synthesis. Hence it is interesting to investigate whether our model is consistent with mechanisms proposed for these reactions.

H_2–D_2 exchange. The model is suitable either for hydrogen–deuterium exchange via an Eley–Rideal mechanism, or via a Bonhoeffer–Farkas mechanism. In fact, for the first mechanism the model offers for all H_2(I) coverages a bare site near this species suitable to weakly polarize a H_2 molecule from the gas phase which could react with the dissociative adsorbed species. Such a pathway has been suggested as the predominant one by Naito *et al.* on ZnO (*26*). The model is also consistent with the Bonhoeffer–Farkas mechanism according to which the exchange takes place when H and D adsorbed atoms are desorbed. Such a pathway has been suggested as the predominant one on ZnO by Conner and Kokes (*35*).

In our model at any H_2(I) coverage both the hydridic and hydroxyl hydrogen partners can independently migrate onto bare adjacent sites. This surface mobility allows an easy recombination of H atoms coming from two different molecules.

Methanol synthesis. It is also interesting to investigate whether our model is suitable

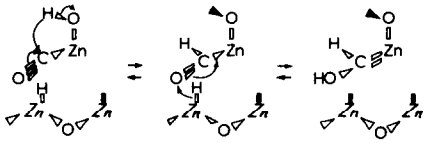

SCHEME VI

to propose a mechanism for methanol synthesis. If we look at Scheme IV, we can see that CO and H_2(I) chemisorbed species are in positions very favorable for making formyl and hydroxycarbene intermediates. A possible scheme for CO(2) and H_2(I) interaction is shown above (Scheme VI). An analogous scheme for CO(3) and H_2(I) interaction can be proposed.

The initial steps of methanol synthesis on ZnO are thus proposed to be the heteropolar splitting of hydrogen and the chemisorption of the CO followed by the electrophilic attack of the carbon end of CO by protons and a nucleophilic attack on the oxygen end of CO by hydride ions. The first attack give rise to formyl intermediates, the second one to hydroxycarbenes. In our model the two attacks can easily take place during the OH and ZnH bending vibrations. A similar mechanism involving formyl and hydrocarbene intermediates has been proposed for the catalytic synthesis of methanol on Cu/ZnO systems (*36*).

ACKNOWLEDGMENTS

We thank the Italian Ministero della Pubblica Istruzione, "Progetti nazionali di rilevante interesse per lo sviluppo della Scienza," for financial support.

REFERENCES

1. Taylor, J. H., and Amberg, C. H., *Canad. J. Chem.* **39,** 535 (1961).
2. Amberg, C. H., and Seanor, D. A., "Proceedings, International Congress on Catalysis, 3rd (Amsterdam, 1964)." Vol. I, p. 450. North-Holland, Amsterdam, 1965.
3. (a) Garrone, E., Ghiotti, G., Giamello, E., and Fubini, B., *J. Chem. Soc., Faraday Trans. I* **77,** 2613 (1981); (b) Giamello, E., and Fubini, B., *J. Chem. Soc., Faraday Trans. I* **79,** 1995 (1983).
4. Kortum, G., and Knehr, H., *Z. Phys. Chem. Neue Folge* **89,** 194 (1974).
5. Dent, A. L., and Kokes, R. J., *J. Phys. Chem.* **73,** 3772 (1969).
6. Boccuzzi, F., Garrone, E., Zecchina, A., Bossi, A., and Camia, M., *J. Catal.* **51,** 160 (1978).
7. Nagarjunan, T. S., Sastri, M. V. C., and Kuriacose, J. C., *J. Catal.* **2,** 223 (1963).
8. Aharoni, C., and Tompkins, F. C., *Trans. Faraday Soc.* **66,** 434 (1970).
9. Tsuchiya, S., and Shiba, T., *Bull. Chem. Soc. Japan* **41,** 573 (1968).
10. Giamello, E., and Fubini, B., *in* "Adsorption at the Gas–Liquid Interface" (J. Rouquerol and K. S. W. Sing, Eds.), p. 389. Elsevier, Amsterdam, 1982.
11. Boccuzzi, F., Borello, E., Zecchina, A., Bossi, A., and Camia, M., *J. Catal.* **51,** 150 (1978).
12. Fubini, B., Giamello, G., Della Gatta, G., and Venturello, G., *J. Chem. Soc., Faraday Trans. I* **78,** 153 (1982).
13. (a) Griffin, G. L., and Yates, J. T., Jr., *J. Chem. Phys.* **77,** 3744 (1982); (b) Griffin, G. L., and Yates, J. T., Jr., *J. Chem. Phys.* **77,** 3751 (1982).
14. Lavalley, J. C., Saussey, J., and Rais, T., *J. Mol. Catal.* **17,** 289 (1982).
15. Zecchina, A., Ghiotti, G., Cerruti, L., and Morterra, C., *J. Chim. Phys.* **68,** 1479 (1971).
16. Ghiotti, G., Garrone, E., Morterra, C., and Boccuzzi, F., *J. Phys. Chem.* **83,** 2863 (1979).
17. Zecchina, A., Garrone, E., Ghiotti, G., and Coluccia, S., *J. Phys. Chem.* **79,** 972 (1975).
18. Lubezky, A., and Folman, M., *Trans. Faraday Soc.* **67,** 3110 (1971).
19. Gay, R. R., Nodine, M. H., Henrich, V. E., Zeiger, H. J., and Solomon, E. I., *J. Amer. Chem. Soc.* **102,** 6752 (1980).
20. McClellan, M. R., Trenary, M., Shin, N. D., Sayers, M. J., D'Amico, K. L., Solomon, E. I., and McFeely, F. R., *J. Chem. Phys.* **74,** 4726 (1980).
21. Boccuzzi, F., Borello, E., Chiorino, A., and Zecchina, A., *Chem. Phys. Lett.* **61,** 617 (1979).
22. (a) Boccuzzi, F., Morterra, C., Scala, R., and Zecchina, A., *J. C. S., Faraday Trans. II* **77,** 2059 (1981); (b) Boccuzzi, F., Ghiotti, G., and Chiorino, A., *Faraday Trans. II* **79,** 1779 (1983).
23. Atherton, K., Newbold, G., and Hockey, J. A., *Disc. Faraday Soc.* **52,** 33 (1971).
24. Morishige, K., Kittaka, S., Moriyasu, T., and Morimoto, T., *J. C. S. Faraday* I **76,** 738 (1980).
25. Dent, A. L., and Kokes, R. J., *J. Phys. Chem.* **73,** 3772 (1969).
26. Naito, S., Shimizu, H., Hagiwara, E., Onishi, T., and Tamaru, K., *Trans. Faraday Soc.* **67,** 1515 (1971).
27. Kokes, R. J., Dent, A. L., Chang, C. C., and Dixon, L. T., *J. Amer. Chem. Soc.* **34,** 4429 (1972).
28. Bellamy, L. J., in "The Infrared Spectra of Complex Molecules," Vol. 2, pp. 95, 118. Chapman & Hall, London, 1980.

29. Saussey, J., Lavalley, J. C., and Bovet, C., *J. C. S. Faraday Trans. I* **78,** 1457 (1982).

30. Cheng, W. H., and Kung, H. H., *Surface Sci.* **122,** 21 (1982).

31. Pasquali, M., Floriani, C., and Gaetani-Manfredotti, A., *Inorg. Chem.* **19,** 1191 (1980).

32. Bell, N. A., Moseley, P. T., Shearer, H. M. M., and Spencer, C. B., *J. C. S. Chem. Comm.* 359 (1980).

33. John, C. S., *in* "Catalysis," Vol. 3, p. 169. Chem. Soc., London, 1980.

34. Hirschwald, W., *in* "Current Topics in Materials Science," Vol. 7, p. 448. North-Holland, Amsterdam, 1981.

35. Conner, W. C., Jr., and Kokes, R. J., *J. Catal.* **36,** 199 (1975).

36. Herman, R. G., Klier, K., Simmons, G. W., Finn, B. P., Bulko, J. B., and Kobylinski, T. P., *J. Catal.* **56,** 407 (1979).